Surface Morphology of Copper Deposits by Using Azine Derivatives on an Ecofriendly Electroless Bath

P. BalaRamesh[a,*], P. Venkatesh[b]

[a] *Department of Chemistry, RMK Engineering College, Chennai, Tamilnadu, India,*
[b] *Department of Chemistry, Pachaiyappa's College, Chennai, Tamilnadu, India,*
[*] *e-mail: balarameshp@gmail.com; pbr.sh@rmkec.ac.in*

This article reports the effect of azine stabilizers such as pyridine, 2,2'-bipyridine and 1,10-phenanthroline during electroless deposition of copper. In this work, the biodegradable copper methanesulphonate was used instead of the traditionally used copper sulphate and the environmentally safe polyhydroxylic compound xylitol was used as the complexing agent. Commercial paraformaldehyde was used as the reducing agent and potassium hydroxide (KOH) was used to optimize the bath in alkaline medium at pH 13.25. Surface morphologies of the electroless coated copper (Cu) substrates were investigated by atomic force microscopic (AFM) analysis. Crystallite size and specific surface area of copper thin film were observed by x-ray diffraction (XRD). Electrochemical characteristics were studied by cyclic voltammetry (CV) and Tafel polarization. The value of charge transfer resistance and double layer capacitance were determined by impedance techniques. In this xylitol bath, 2,2'-bipyridine was found to act as an enhancer but the results are not very different from the plain xylitol bath. Pyridine acted as a strong inhibitor and 1,10-phenanthroline was a good accelerator. All stabilizers provide high stability to the bath at 28 ± 2°C with 1 ppm addition.

Keywords: azine stabilizers, copper methanesulphonate, crystallite size, surface morphology, xylitol.

УДК 669.2.8+669.1(047)

INTRODUCTION

Electroless plating is an autocatalytic process that is being increasingly thought to be more useful than electroplating for the deposition of metal coatings and films because of improvements in solution stability, possibility of producing coatings with uniform thickness, capability of depositing material even in deep recesses, bores, blind holes, high selectivity, possibility of producing very thin layers, excellent step coverage, good filling capacity and absence of need for electrical contacting of wafers during deposition.

Although the method for polishing and silvering plates for looking glasses/mirrors was described as early as 1798 by S. Bernard [1], the first scientific description of the electroless deposition process may be attributed to German chemist Justus Von Liebig in 1835. Von Leibig reported the reduction of silver salts to silver metal on glass surface, can be done by using an aldehyde as the reducing agent [2]. In 1844, Wurtz [3] observed that Ni^{2+} ions can be reduced by hypophosphite ions, what is now recognized as the "electroless process". However, he obtained only a black powder.

The initial formulation of electroless plating is credited to Brashear in 1880 [4]. This discovery can be considered as the official pioneer of the electroless deposition process. In 1900, D.F. Weiskopf and in 1907, F.D. Chattway plated copper on glass from a solution containing copper and formaldehyde [5, 6]. Since then, electroless coatings have been reported by many workers such as P. Breteau (1911), A. Silvermann (1915) and F.A. Roux (1916) [7–9]. Controlled electroless plating process was accidently discovered by Brenner and Riddell in 1946 [10], when they tried to electroplate Ni-W alloy on the inner side of a steel tube using a citrate bath.

In 1947, Narcus [11] reported and established an optimum plating condition for electroless plating. The first commercial applications of electroless deposition were reported by A. Brenner (1959), Cahill, (1957) and Wein, (1959) [12], [13]. The theoretical basis of electroless copper deposition process has been studied by Pearlstein, in Lowenheims book reviewed by Saubestre, (1962), Zeblisky, (1963), Lukes, (1964) and Goldie, et al., (1964) [14–17].

The advantages of electroless plating have resulted in considerable research being conducted in the field in recent years [18–21]. Of the forty six different processes regulated under metal finishing standards featuring different technologies, operational steps, inputs, and outputs, electroless copper plating has found widespread acceptance in many applications such as in the fabrication of decorative articles, semiconductors, integrated circuits and through-hole plating in printed circuit boards [22–25].

In 1966, M. Saito [26] reported that compounds having planar and other structures with lone pairs of electrons such as sulphur and nitrogen containing hetero-organic compounds have been proposed as stabilizers. These additives on copper surface

© BalaRamesh P., Venkatesh P., Электронная обработка материалов, 2015, **51**(6), 55–60.

decrease the plating rate, delocalized π-electron enhances the plating rate and stronger the complexing ability of additives with copper (I) than with copper (II) stabilizer will be solution.

Xylitol has been proposed as ecofriendly chelating agent to be used in methanesulphonic acid (MSA) baths because it forms sufficiently stable complexes with copper (II) ions in alkaline solutions. In this work, we report the texture of surface morphology of copper deposits formed by electroless deposition from copper methanesulphonate, xylitol baths with pyridine, 2,2'-bipyridine and 1,10-phenanthroline as stabilizers. Use of these stabilizers results in electroless copper deposits as established by AFM, CV, Tafel, and XRD testing.

1. EXPERIMENTAL

An environmentally friendly bath for electroless deposition of copper was prepared using methanesulphonate, xylitol, para-formaldehyde, potassium hydroxide (to vary the pH of the bath), pyridine, 2,2'-bipyridine and 1,10-phenanathroline are given in Table 1. The electroless copper deposition was performed on a copper sheet (2.0 × 2.0 × 0.1 cm) in a 100 mL beaker. Before deposit, the copper substrate was rinsed with double distilled water after polishing with fine grid paper. A scoring process was used to clean the precleaned substrates using KOH solution. After rinsing with distilled water, surface etching was performed using a solution of $KMnO_4$ and H_2SO_4 to remove any oxidised layer on the surface. In order to improve the deposition rate and adhesive properties of the copper thin film, the surface was sensitized using $SnCl_2$ solution ($SnCl_2$ mixed with HCl) and activated using HCl solution of $PdCl_2$.

Table 1. Bath composition of copper methanesulphonate xylitol plain bath with stabilizers

Bath contains	Plain bath	Stabilizers used bath
CuMS (II) ion contacting salt	3 g/L	3 g/L
Xylitol	20 g/L	20 g/L
HCHO	10 g/L	10 g/L
KOH (pH)	13.25	13.25
Temperature	28 ± 2ºC	28 ± 2ºC
Stabilizers (pyridine, 2,2'-bipyridine and 1,10-phenanthroline)	0 ppm	1 ppm

About 50 g of copper carbonate was weighed and transferred into 500 mL beaker. The copper carbonate was treated with 60 mL of methanesulphonic acid until the evolution of CO_2 gas, and made up to 250 mL, using double distilled water. The solution was filtered to remove all visible impurities and stored in a standard measuring flask. The amount of copper present in the stock solution was evaluated by adding 0.1N standard sodium thiosulphate solution to 1 mL of the stock solution and weighting the copper deposited. All measurements were repeated at least thrice.

The properties of the electroless copper thin film were studied. X-ray diffraction (XRD) (X'Pert-Pro, P-analytical) was used to identify the structural properties such as crystallite size and quality of the plated copper. The surface topography was evaluated using atomic force microscope (AFM) (Nano-Surf Easy Scan2, Switzerland) and the surface roughness of the copper deposit was analysed. Cyclic voltammetric curves were obtained by standard electrochemical analyser CHI 600D Austin USA. The copper methanesulphonate solution was deaerated with nitrogen gas. The counter electrode was platinum wire and reference electrode was Ag/AgCl with saturated KCl solution. The voltammograms were recorded at room temperature 28 ± 2ºC in 0.1M Na_2SO_4 as supporting electrolyte. Standard glassy carbon electrode was used as working electrode and the voltammograms was recorded in the range from -1.2 to +0.5 V at potential scanning rate 50 mV/s.

2. RESULTS AND DISCUSSION

2.1. Calculation for rate and thickness of copper deposits

Electroless copper deposition was found to start at pH of 12.5 in xyllitol bath, the rate of deposition increased initially and then decreased with further increases in pH. Through iterative experiments, the bath compositions were optimized, the bath containing 3 g/L of copper methanesulphonate and 10 g/L of para-formaldehyde was taken as the optimum formulation. The xylitol bath showed an optimum deposition rate of 3.24 μm/h at pH 13.25.

The rate of deposition "*T*" was calculated using the following relation. All measurements were repeated at least thrice. The rate of deposition "*T*" was calculated using the following relation:

$$T = W \cdot 10^4 / D\,At. \qquad (1)$$

Where, "*W*" is the mass of the deposit (g), "*D*" is the density of the film material (g/cm^3), "*A*" is the area of the film coated (cm^2) and "*t*" is the coating duration (*h*).

After electroless plating, the panel was washed, rinsed, dried and weighed (w_1). The electroless copper coating was dissolved in 10–20% HNO_3 solution. The panel was then washed, rinsed, dried and weighed (w_2). The actual weight of the deposit was calculated from the difference in weight before and after plating ($w_1 - w_2$). From the weight of the deposit, total plated area and density of the copper, thickness was calculated as follows.

$$Thickness\,(\mu m) = \frac{W \cdot 10^4 \cdot 60}{A \times D} \qquad (2)$$

where, $W = (w_1 - w_2)$ = Weight of deposit in gram; w_1 = Weight after plating; w_2 = Weight after stripping; A = Total plated area of the substrate (cm^2); D = Density of the copper (g/cm^3).

Table 2. Deposition rate and thickness of copper deposits on optimized methanesulphonate xylitol plain bath with stabilizers

S. No.	Xylitol plain bath with stabilizers (1 ppm)	Deposition rate (µm/h)	Thickness (µm)
1	Plain bath	3.23	193.8
2	Pyridine	2.53	151.8
3	2,2'-bipyridine	3.56	213.6
4	1,10-Phenanthroline	3.73	223.8

The inhibiting or accelerating properties of the stabilizers were compared in terms of the deposition rate (µm/h) of the electroless plating plain bath. Table 2 shows that, when the rates of deposition values were lower than that of plain bath, the stabilizers were considered to be inhibitors and when greater, as accelerators or enhancers.

2.2. Nanostructure – Atomic force microscope (AFM)

Bright copper deposits seen in atomic force microscopy (AFM) indicate better mechanical and physical properties. Roughness values are inversely propositional to smooth deposition. Table 3 and Fig. 1 indicates the roughness values of the xylitol plain bath and bath with the three stabilizers. The xylitol plain bath produced maximum roughness value of 303 nm. On using stabilizers the roughness values decreased until 2,2'-bipyridine due to steric factors then increased to 1,10-phenanthroline.

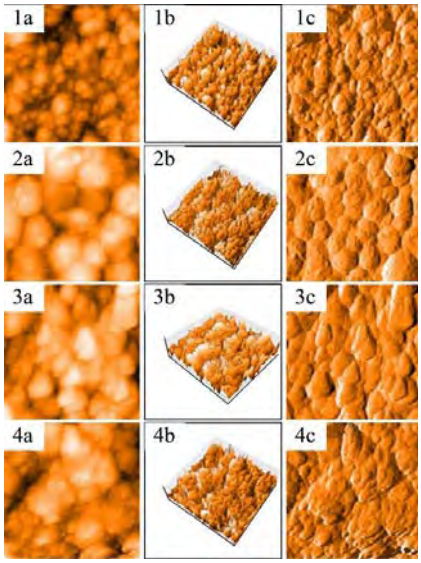


Fig. 1. AFM images of copper deposits on methanesulphonate xylitol plain bath; topography of copper deposits (a), 3-D image (b) and surface area (c); xylitol plain bath (1a, 1b, 1c), pyridine bath (2a, 2b, 2c), 2,2'-bipyridine (3a, 3b, 3c), 1,10-phenanthroline bath (4a, 4b, 4c).

Table 3. Roughness value of copper deposits on xylitol methanesulphonate plain bath with stabilizers from AFM studies

S. No.	Xylitol plain bath with stabilizers (1 ppm)	Roughness value (nm)
1	Plain bath	303
2	Pyridine	156
3	2,2'-bipyridine	69
4	1,10-Phenanthroline	92

2.3. Quality and quantity – Cyclic voltammetry (CV)

The inhibiting and enhancing properties of stabilizers can be understood from the anodic peak current value, anodic peak potential value and peak appearance. Based on cyclic voltammetry studies, the inhibiting properties of the stabilizer result in low anodic peak potential values. The low-energy oxidation process is enhanced by stabilizers. Figure 2 and Table 4 shows that the appearances of the sharp peaks indicate that the rate of oxidation is high. The high anodic peak current value also indicates that the stabilizer inhibits the deposition of copper. The low anodic peak current, high peak potential and broad peaks indicate the enhancing properties of the stabilizers.

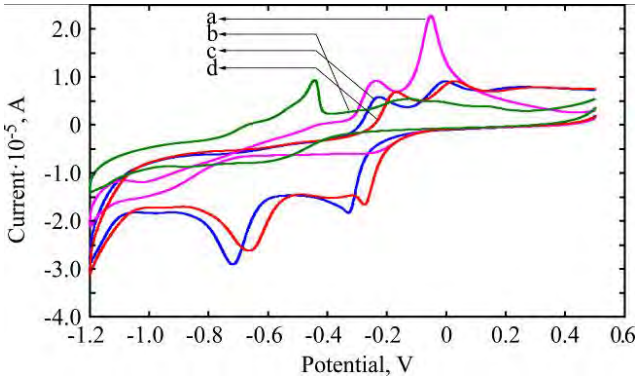


Fig. 2. Cyclic voltammogram for electroless copper methanesulphonate xylitol bath at pH 13.25; 2,2'-bipyridine bath (a), 1,10-phenanthroline bath (b), xylitol plain bath (c), pyridine bath (d).

Table 4. Anodic peak potential and anodic peak current values from cyclic voltammogram for electroless copper methanesulphonate xylitol plain bath with stabilizers

S. No.	Xylitol plain bath with stabilizers (1 ppm)	$E_{pa\text{-}1}$ values (mV)	$I_{pa\text{-}1}$ values (mA)
1	Plain bath	-0.2275	$5.924 \cdot 10^{-6}$
2	Pyridine	-0.4423	$9.355 \cdot 10^{-6}$
3	2,2'-bipyridine	-0.1987	$2.980 \cdot 10^{-6}$
4	1,10-Phenanthroline	-0.1200	$6.251 \cdot 10^{-5}$

2.4. AC electrochemical monitoring technique – Electrochemical impedance spectroscopy (EIS)

The inhibiting and accelerating properties can also be seen from the higher and lower resistance

values respectively, compared to the xylitol pain bath. The Table 5 and Fig. 3 indicates that pyridine shows the highest resistance value confirming the inhibiting properties. 1,10-phenanthroline shows good acceleration effects. 2,2'-bipyridine acted as accelerator but the results are closer to xylitol plain bath.

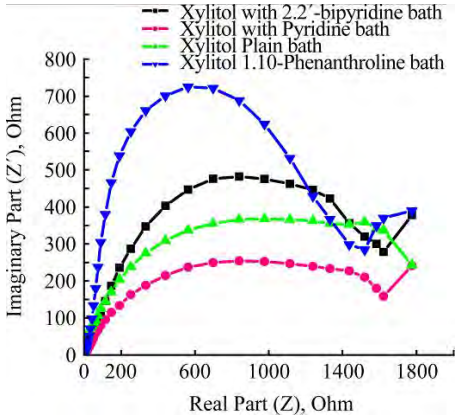


Fig. 3. Nyquist diagram of electroless copper methanesulphonate xylitol bath in pH 13.25.

The following electrical equivalent circuit was found to match the system

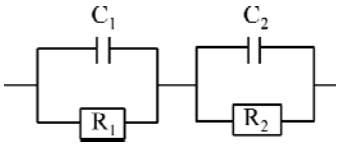


Fig. 4. Electrical equivalent circuits for electrochemical impedance spectroscopy.

where, C_1 & C_2 – Double layer capacitances; R_1 & R_2 – Charge transfer resistances

$$\frac{C_1}{R_1}+\frac{C_2}{R_2}. \tag{3}$$

Nyquist diagram {*Im* (*Z*) Vs Re (*Z*')}

$$fc_1=\frac{1}{2\pi R_1 C_1} \text{ and } fc_2=\frac{1}{2\pi R_2 C_2}. \tag{4}$$

Figure 4 show that two resistance and capacitance values namely C_1, C_2 and R_1, R_2 were obtained by the following equivalent circuit.

Order $C_1 < C_2$.

Table 5. Electrochemical impedance value of charge transfer resistance and double layer capacitance for electroless copper methanesulphonate xylitol plain bath with stabilizers

S. No.	Xylitol plain bath with stabilizers (1 ppm)	Double layer Capacitance (C_{dl}) (C_{dl}) (μF/cm^2)		Charge transfer Resistance (R_t) (mΩ/cm^2)	
		$C_1 \cdot 10^{-6}$	$C_2 \cdot 10^{-3}$	R_1	R_2
1	Plain bath	3.474	0.1421	256	30.23
2	Pyridine	6.576	0.4706	554	75.12
3	2,2'-bipyridine	2.068	0.0916	245	24.52
4	1,10-Phenanthroline	2.309	0.1131	352	15.94

2.5. DC electrochemical monitoring technique – Tafel polarization (TP)

Ohno et al., [27] showed that the rate of copper deposits can be determined using deposition current values obtained from the Tafel plots. The copper deposition rate can be calculated using the following "the American Society for Testing and Materials" standard equation.

Corrosion current, corrosion potential, deposition rate for electroless copper methanesulphonate xylitol plain bath with stabilizers and the results are given in Fig. 5 and Table 6.

$$deposition\,rate\,(\mu m/h)= \\ =3.7328\times10^{-4}\left[\frac{i_{dep}}{D}\right]\times Eq.wt \tag{5}$$

where, i_{dep} = Deposition current; D = Density of the copper metal (g/cm^3); Eq. wt = Equivalent weight of the copper metal.

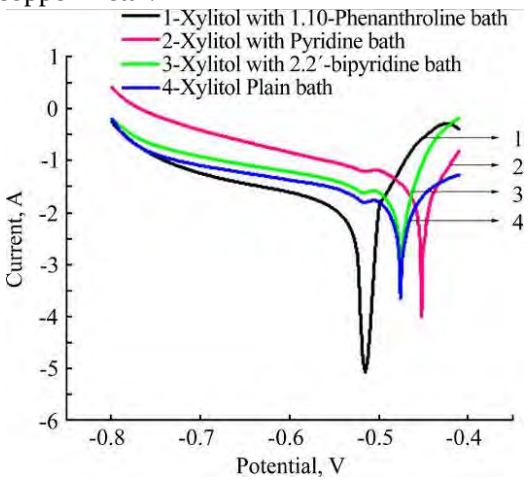


Fig. 5. Tafel polarization curve for electroless copper methanesulphonate xylitol bath pH 13.25.

2.6. Phase composition – X-ray diffraction (XRD)

The crystal orientations and lattice parameters were studied by XRD. Lee et al., [28] have earlier reported that copper methanesulphonate bath results in large quantities of copper ions, because of high conductivity and solubility leading to (200) plane. The crystallite size of the copper deposits can be estimated by using Debye-Scherrer's equation [29, 30].

$$\rho = K\lambda/\beta\cos\theta \tag{6}$$

where, K is the Scherrer constant, "λ" is the wavelength of light used for the diffraction, "β" is the "Full Width at Half Maximum" of the sharp peaks and θ is the angle measured. The Scherrer constant (K) in the above formula accounts for the shape of the particle and is generally taken to have the value 0.89.

Specific surface area of the copper deposits is determined by the formula

$$S=\frac{6\times10^3}{D\rho} \tag{7}$$

where, "ρ" is the crystallite size (nm) and "D" is the theoretical density of copper (8.96 g/cm^3).

Table 6. Tafel polarization value of corrosion current, corrosion potential and deposition rate for electroless copper methanesulphonate xylitol plain bath with stabilizers

S. No.	Xylitol plain bath with stabilizer (1 ppm)	β_a mV/decade	β_c mV/decade	E_{corr} (mV)	I_{corr} (mA)	Deposition rate (μm/h)
1	Plain bath	51.30	247.7	- 441.77	41.01	0.543
2	Pyridine	84.91	263.7	- 456.61	16.39	0.217
3	2,2'-bipyridine	115.0	308.7	- 502.07	53.84	0.713
4	1,10-Phenanthroline	109.2	82.76	- 558.62	87.21	1.154

Crystallite sizes are proportional to the inhibiting efficiency. Figure 6 and Table 7 shows that crystallites were larger for pyridine, indicating inhibiting effect of this stabilizer in the xylitol plain bath. But, 2,2'-bipyridine and 1,10-phenanthroline were found to have better results than the plain bath. Baths with pyridine to 1,10-phenanthroline resulted in a decrease in crystallite size.

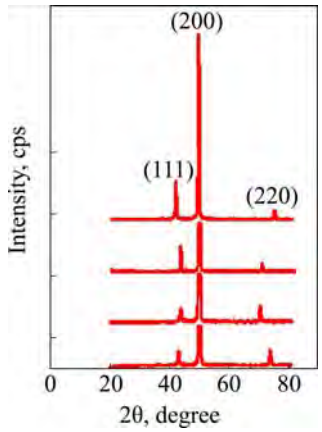


Fig. 6. XRD pattern of copper deposits on methanesulphonate xylitol plain bath with stabilizers (1 ppm).

Table 7. Crystallite size and specific surface area of copper deposits for electroless copper methanesulphonate xylitol plain bath with stabilizers

S. No	Xylitol plain bath with stabilizers (1 ppm)	Crystallite size (nm)	Specific surface area (m^2/g)
1	Plain bath	126	5.315
2	Pyridine	158	4.238
3	2,2'-bipyridine	123	5.444
4	1,10-Phenanthroline	112	5.979

3. CONCLUSIONS

Deposition rate and micro thickness of the copper deposits were found to increase from pyridine to 1,10-phenanthroline. This can be attributed to the size, charged ion characteristics, complexation of stabilizers, and effect of delocalized π-electron present in heteroatoms, such as sulphur and nitrogen. Surface roughnesses of copper deposits were observed by atomic force microscope technique. The complexation and steric factors of stabilizers may have altered the roughness value. Xylitol based methanesulphonate baths produced bright deposits.

Intensity counts, position of 2-theta and "full width at half maximum" values were obtained by x-ray diffraction studies. Crystallite size and specific surface area of electroless copper deposits were calculated by using Debye-Scherer's equation. Because of high conductivity and solubility of copper methanesulphonate, the deposits of copper oriented in the (200) plane.

To understand the electrochemical role of the stabilizers in electroless copper deposition, cyclic voltammetry studies were performed. The quality of copper was determined by anodic peak potential (E_{pa} – value) and quantity of the copper deposits was determined from the anodic peak current value (I_{pa} – value). The cyclic voltammetry data confirmed that the inhibiting properties decreased from pyridine to 1,10-phenanthroline.

Electrochemical interfacial charge transfer between copper substrate and electroless copper methanesulphonate bath was studied using impendance measurements. Resistance value increased from pyridine to 1,10-phenanthroline, and capacitance value was lower than the xylitol plain bath.

The three organic azine compounds studied are found to greatly stabilize the bath and extend its life. They were found to modify the crystal structure with the production of compact, dense, and high etching resistant deposits. The physical and electrochemical data clearly indicates that the xylitol bath produces copper deposits that are finer and more compact. Moreover, smooth and shiny deposits were obtained on using 2,2'-dipyridyl to xylitol bath.

REFERENCES

1. Bernard S. Description de la Maniere Dont se Polissent et s'etament Les Glaces Coulees Dans l'atelier au Foubourg Antoine. *J de 1'ficole Polytechnique*. 1798, **2**(5), 71–81.
2. Justus Von Liebig. About the Products Fecit Alcohol, Aldehyde. *Annual Review of Pharmacology*. 1835, **14**, 134.
3. Wurtz A. On the Copper Hydride. *Annals of Chemistry and Physics*. 1844, **3**, 11.
4. Brashear H. Hints on Silvering Specula, & c'. *England in Mechanical*. 1880, **31**, 327.
5. Weiskopf D.R., & Co. *Process for Making Copper Mirror*. D.R.P. No-124. 1900, pp. 710.
6. Chattway F.D. Copper Mirrors. *P Roy Soc Lond A Mat*. 1907, **80**, 88–92.
7. *Notice sur les travaux scientifiques de M. Pierre Breteau*. Paris: Gauthier–Villars, 1911, 26 p.

8. Silvermann A. The Silvering of Glass. *Transactions of the American Ceramic Society*. 1915, **17**, 505–519.

9. Roux F.A. *Process for Producing Metal Deposits*. U.S. Patent 1207218, issued December 5, 1916.

10. Brenner A.R., and Riddell G.E. Nickel Plating on Steel by Chemical Reduction. *J Res Natl Bur Stand.* 1946, **37**, 31–34.

11. Narcus H. Practical Copper Reduction on Nonconductors. *Met Finish.* 1947, **45**, 64–67.

12. Cahill A.E. Surface Catalyzed Reduction of Copper. *American Electrochemical Society Proceedings.* 1957, **44**, 130.

13. Wein S. *Silvering Process and Materials*. US Patent 2871139, issued January 27, 1959.

14. Saubestre E.B. Electroless Plating Today. *Met Finish*. 1962, **60**, 17.

15. Zeblisky R.J., McCormack J.F., Williamson J.D., and Shneble F.W. *Electroless Copper Plating.* U.S. Patent 3095309 A, issued June 25, 1963.

16. Lukes R.M. The Chemistry of the Autocatalytic Reduction of Copper by Alkaline Formaldehyde. *Plating.* 1964, **51**, 1066–1068.

17. Goldie W. Electroless Copper Deposition. *Plating*. 1964, **51**, 1069–1074.

18. Norku E., Prusinskas K., Vaskelis A., Jaciauskiene J., Stalnioniene I., and Macalady D.L. Application of Saccharose as Copper (II) Ligand for Electroless Copper Plating Solutions. *Carbohyd Res*. 2007, **342**, 71–78.

19. Schlesinger M., and Paunovic M. *Modern Electroplating*. 4th edition. New York: John Wiley, 2000. 868 p.

20. Schlesinger M., and Paunovic M. *Modern Electroplating*. 5th Edition. New York: John Wiley, 2010. 736 p.

21. Balaramesh P., Venkatesh P., Rekha S., and Hemamalini M. Bath Parameters Affecting Electroless Copper Deposition-A Review. *International J of Innovative Research and Studies*. 2014, **3**, 167–181.

22. Hanna F., Hamid F.A., and Aal A.A. Controlling Factors Affecting the Stability and Rate of Electroless Copper Plating. *Mater Lett*. 2003, **58**, 104–109.

23. Balci S., Bittner A.M., Hahn K., Scheu C., Knez M., Kadri A., Wege C., Jeske H., and Kern K. Copper Nanowires Within the Central Channel of Tobacco Mosaic Virus Particles. *Electrochim Acta*. 2006, **51**, 6251.

24. Cho Sang Jin, Nguyen Trieu, and Boo Jin Hyo. Polyimide Surface Modification by Using Microwave Plasma for Adhesion Enhancement of Copper Electroless Plating. *JNN*. 2011, **11**, 5328–5333.

25. Guo R.H., Jiang S.X., Yuen C.W.M., Ng M.C.F., Lan J.J.W., Yeung Y.L., and Lin S.J. Effects of Deposition Parameters of Electroless Copper Plating on Polyester Fabric. *Fiber and Polymer*. 2013, **14**, 752–758.

26. Saito M. Effect of the Main Conditions of Chemical Copper Plating on its Local Anode Reaction and Cathode Reaction Electrochemical Studies on Chemical Copper Plating (II). *J of the Metal Finishing Society of Japan*. 1966, **17**(1), 14–19.

27. Ohno I., Wakabayshi O., and Haruyama S. Anodic Oxidation of Reluctant in Electroless Plating. *J Electrochem Soc*. 1985, **132**, 2323–2330.

28. Lee D.N. Texture and Related Phenomena of Electrodeposits. *J of Korean Institute of Surface Engineering*. 1999, **32**, 317–330.

29. Debye P., and Scherrer P. Interference of Irregularly Oriented Particles in x-rays. *Physical J*. 1916, **17**, 277–283.

30. Cullity B.D. *Element of X-ray diffraction*. 2nd edition. London: Addison-Wesley, 1978. pp. 101–103.

Received 23.03.15
Accepted 14.04.15

Реферат

В статье рассматривается влияние на химическое осаждение меди азиновых стабилизаторов, таких как пиридин, 2,2'-бипиридин и 1,10-фенантролин. В этой работе вместо традиционно используемого сульфата меди использовали биоразлагаемый метансульфонат меди и в качестве комплексообразующего агента было использовано экологически безопасное полигидроксильное соединение – ксилит. Коммерческий параформальдегид был использован в качестве восстанавливающего агента и гидроксид калия (KOH) был использован для обеспечения оптимальной щелочности ванны с pH 13,25. Морфология поверхности химически осажденного покрытия на медном (Cu) субстрате была проанализирована с помощью атомно-силовой микроскопии (АСМ). Размер кристаллитов и удельная площадь поверхности тонкой медной пленки определялась методом рентгеновской дифракции (XRD). Электрохимические характеристики были изучены с помощью циклической вольтамперометрии (CV) и Тафелевской поляризации. Величины сопротивления переноса заряда и емкости двойного слоя были определены импедансным методом. Было установлено, что в этой ванне с ксилитом, 2,2-бипиридин действует в качестве усилителя, но результаты не очень отличается от простой ванной с ксилитом. Пиридин действует как сильный ингибитор, но 1,10-фенантролин был хороший ускоритель. Все стабилизаторы обеспечивают высокую устойчивость ванны при 28 ± 2°C при добавке в количестве 1 промилле.

Ключевые слова: азиновые стабилизаторы, метансульфонат меди, размер кристаллитов, морфология поверхности, ксилит.